Accurate Fault Location in AC/DC Hybrid Line Corridors Based on Eigenvalue Decomposition

Dayou Lu[1], *Student Member*, *IEEE*, Yu Liu[1,2,*], *Member*, *IEEE*, Wentao Huang[2,3], *Member, IEEE* and Xinze Xi[4,5]
1. School of Information Science and Technology, ShanghaiTech University, Shanghai, China, 201210;
2. Key Laboratory of Control of Power Transmission and Conversion, Ministry of Education, Shanghai, China, 200240
3. Department of Electrical Power Engineering, Shanghai Jiao Tong University, Shanghai, China, 200240
4. School of Electrical Engineering, Chongqing University, Chongqing, China, 400044
5. Electric Power Research Institute of Yunnan Power Grid Co., Ltd, Kunming, Yunnan, China, 650217
*Email: liuyu.shanghaitech@gmail.com

Abstract: Accurate fault location algorithm minimizes the fault searching time and operating cost. This paper proposes an accurate fault algorithm for untranposed multi-phase AC/DC hybrid line corridors in time domain. The proposed method considers the distributed line parameter and applies the eigenvalue decomposition to decouple the system. The Bergeron model is applied to solve the voltage distribution through the line to achieve the fault location. Numerical experiments in a five-phase AC/DC system with only 5 ms data window prove that the proposed method presents higher fault location accuracy compared to fault location results without considering the mutual coupling effects between AC and DC systems, independent of fault types, locations and impedances.

Key words: fault location, AC/DC hybrid line corridor, eigenvalue decomposition, Bergeron model

I. INTRODUCTION

ACCURATE fault location algorithm for transmission lines reduces the time spent searching for the fault and saves the operating cost for power systems [1-4]. With the increasing demand for the electric power, the transmission line corridors are widely applied. The transmission line corridors are constructed with the parallel lines on the same tower that allow the power transmission of high voltage classes, and with the parallel lines on nearby towers based on the economic and environmental concern. For example, the two-circuit parallel lines (with number of phase conductors greater than three) may include: two three-phase AC lines in parallel (AC/AC), two double-pole DC lines in parallel (DC/DC), and one three-phase AC line paralleled with one double-pole DC line (AC/DC). To achieve accurate fault location in the line corridors, the techniques of modal decomposition that decouple the high dimensional system into several independent single-mode transmission lines are typically applied. In recent literatures, the techniques of modal decomposition mostly depend on certain assumptions of the phase number and the structure of the line parameter matrix, which treat the AC/AC, DC/DC and AC/DC lines differently.

For the transmission line corridors constructed with two AC lines in parallel, various fault location algorithms have been proposed [5-9]. Phasor domain methods are firstly proposed for these problems. A one-terminal impedance method is proposed with assumption of transposed lines in [5]. A multi-terminal method with the lumped parameter line model is proposed in [6]. With the improvement of the modeling accuracy of transmission lines, a two-terminal method considering the distributed parameters with six-dimensional sequence decomposition is proposed in [7]. In addition, a method uses the eigenvalue decomposition to decouple untransposed lines is proposed in [8]. With short available data window, time domain methods are also proposed. Literature [9] proposes a method that applies a certain constant transform matrix to decouple the six-dimensional system into two three-dimensional systems. For each three-dimensional system, the Clarke transformation with the assumption of transposed line and the Bergeron model are utilized to achieve the fault location.

With the construction of the first actual parallel DC transmission line corridor in practice, the behavior of the electric field for such system is studied in [10] but not the fault location. In [11], the fault location method for such system is proposed, which applies a constant decomposition matrix as well as the eigenvalue decomposition method to decouple the transposed and untransposed four-phase (four-pole) transmission lines, respectively. The Bergeron model is applied to achieve the fault location. Traveling wave based methods are also applied for fault location in parallel DC line corridors [12, 13]. Both literatures adopt the same constant matrix in [11] to decouple the system, and then use the traveling wave methods for fault location.

The AC line and DC line in parallel result in five-phase (three phases and two poles) transmission line corridor or even higher dimensional system (eg. each line consists of parallel circuits on the same tower). Researchers broadly study the behavior of such systems [14-17]. Literature [14] gives a real life example of the AC line and DC line run in parallel. Literatures [14, 15] study the behavior of the five-phase system through calculation of the electromagnetic field and conclude that the variational voltage in AC line could influence the electromagnetic behavior in DC line especially during system transients. Literature [16] studies the influence of the DC line on the AC line by considering the DC bias and second harmonic components on the AC side with the method of circuit theory. Literature [17] studies the secondary arc current on AC side when the faults occur inside DC line, with an approximately adjusted modal decomposition to cover both transposed and untransposed lines, in phasor domain. However, few literatures about fault location for such system are found.

This paper proposes a fault location algorithm for multi-phase untransposed transmission line corridors with distributed parameter modeling in time domain. For untransposed lines in practice, the eigenvalue decomposition can be directly applied for modal decomposition. Therefore, the method does not have certain assumptions of the structure of line parameter matrices or certain phase numbers. Therefore, the proposed algorithm is suitable for various types of corridors. The time domain voltage method based fault location, which claims the location of the fault corresponds to the extremum of the voltage distribution on a transmission line during faults, is applied to locate faults. The Bergeron model [9] is adopted to

This work is sponsored by National Nature Science Foundation of China (No. 51807119), Shanghai Pujiang Program (No. 18PJ1408100) and Key Laboratory of Control of Power Transmission and Conversion (SJTU), Ministry of Education (No. 2015AB04). Their support is greatly appreciated.

978-1-7281-5508-1/20/$31.00 ©2020 IEEEI978-1-7281-5508-1/20/$31.00 ©2020 IEEEE978-1-7281-5508-1/20/$31.00 ©2020 IEEEE978-

solve the voltage distribution through decoupled single-mode transmission lines. Simulation results of fault location with a specific 200 km five-phase AC/DC untransposed transmission line corridor demonstrate that the proposed method achieves higher fault location accuracy compared to the method that neglects the mutual coupling effect between AC and DC circuits, with various fault types, locations and impedances, in 5 ms time window.

The rest of the paper is organized as follows. Section II derives the method to calculate the voltage distribution. Section III shows the fault location algorithm using the voltage method. Section IV exhibits the numerical experiments on the proposed fault location approach. Section V draws a conclusion.

II. Solution of Voltage Distribution for Multi-Phase Transmission Lines

Multi-phase untransposed transmission line corridors with distributed line parameters can always be described with the following M-phase transmission line model in time domain, as shown in Figure 1. k and m are two terminals of the transmission line. The total length of the line is l, and a section of infinitesimal length dx at location x is considered. Matrices $\boldsymbol{R}$, $\boldsymbol{L}$, $\boldsymbol{G}$ and $\boldsymbol{C}$ are the series resistance matrix, series inductance matrix, shunt conductance matrix and shunt capacitance matrix per unit length, respectively. The phase voltages $u_{pj}(x,t)$ and phase currents $i_{pj}(x,t)\,(j=1,2,...,M)$ are defined in the figure.

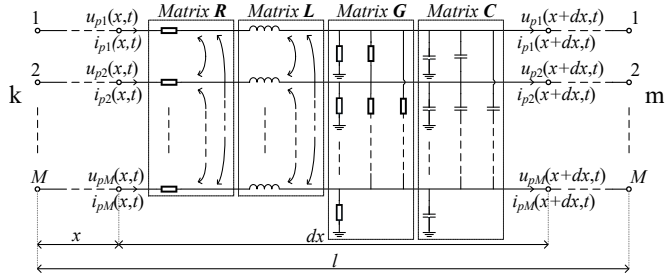

Figure. 1. The *M*-phase transmission line model

From the Kirchhoff's Current Laws (KCLs) and Kirchhoff's Voltage Laws (KVLs), the following partial differential equation set holds,

$$\begin{aligned}\partial \boldsymbol{u}_p(x,t)/\partial x + \boldsymbol{L}\,\partial \boldsymbol{i}_p(x,t)/\partial t + \boldsymbol{R}\boldsymbol{i}_p(x,t) = \boldsymbol{0}\\ \partial \boldsymbol{i}_p(x,t)/\partial x + \boldsymbol{C}\,\partial \boldsymbol{u}_p(x,t)/\partial t + \boldsymbol{G}\boldsymbol{u}_p(x,t) = \boldsymbol{0}\end{aligned} \tag{1}$$

where $\boldsymbol{0}$ is the *M*-dimensional zero vector, $\boldsymbol{u}_p(x,t)=\left[u_{p1}(x,t)\ \cdots\ u_{pM}(x,t)\right]^{\mathrm{T}}$ and $\boldsymbol{i}_p(x,t)=\left[i_{p1}(x,t)\ \cdots\ i_{pM}(x,t)\right]^{\mathrm{T}}$.

The solution of the voltage distribution through the entire transmission line, which is required for voltage method fault location, is equivalent to the solution of $\boldsymbol{u}_p(x,t)$ or the solution of (1). The solution of (1) typically requires the decoupling of (1) into M decoupled equation sets. Afterwards, the Bergeron model can be applied to solve the decoupled equation sets. Therefore, the solution of the voltage distribution of M-phase transmission line corridor includes two steps: step 1 decouples the system into M independent single-mode transmission lines; step 2 uses the Bergeron model to solve the voltage distribution for M decoupled single-phase transmission lines.

A. Modal Decomposition with Eigenvalue Decomposition

For the untransposed line with arbitrary number of the phases and arbitrary structure of the parameter matrices, the first and second equation in (1) cannot be decoupled using same constant eigenmatrix such as the Clarke decomposition. The essence is that matrices $\boldsymbol{L}$ and $\boldsymbol{C}$ cannot be diagonalized with same eigenmatrix. For transmission lines with any phase number and parameter matrix, the only knowledge of $\boldsymbol{L}$ and $\boldsymbol{C}$ is that these matrices are symmetrical matrices (the off-diagonal element $\boldsymbol{L}_{ij}$ equals to $\boldsymbol{L}_{ji}$). With this knowledge, the method of modal decomposition using eigenvalue decomposition can be applied [18]. The basic idea of this method is reviewed and its effectiveness for M-phase transmission line corridor is proved.

For symmetric matrices $\boldsymbol{L}$ and $\boldsymbol{C}$, apply the eigenvalue decomposition to the matrix $\boldsymbol{LC}$,

$$\boldsymbol{T}_u^{-1}\boldsymbol{LC}\boldsymbol{T}_u = \boldsymbol{\Lambda}_{LC} \tag{2}$$

where $\boldsymbol{T}_u$ is the eigenmatrix and $\boldsymbol{\Lambda}_{LC}$ is the diagonal matrix with the eigenvalues of $\boldsymbol{LC}$ as the diagonal elements.

Define $\boldsymbol{T}_i = \left(\boldsymbol{T}_u^{-1}\right)^T$. Take the transposition of (2) with the property of symmetry,

$$\boldsymbol{T}_i^{-1}\boldsymbol{CL}\boldsymbol{T}_i = \boldsymbol{\Lambda}_{LC} \tag{3}$$

Consider the matrix $\boldsymbol{\Lambda}_L = \boldsymbol{T}_i^T\boldsymbol{L}\boldsymbol{T}_i$, one have,

$$\begin{aligned}\boldsymbol{T}_u^{-1}\boldsymbol{LC}\boldsymbol{T}_u\boldsymbol{T}_i^T\boldsymbol{L}\boldsymbol{T}_i = \boldsymbol{T}_i^T\boldsymbol{LCL}\boldsymbol{T}_i = \boldsymbol{\Lambda}_{LC}\boldsymbol{\Lambda}_L\\ \boldsymbol{T}_i^T\boldsymbol{L}\boldsymbol{T}_i\boldsymbol{T}_i^{-1}\boldsymbol{CL}\boldsymbol{T}_i = \boldsymbol{T}_i^T\boldsymbol{LCL}\boldsymbol{T}_i = \boldsymbol{\Lambda}_L\boldsymbol{\Lambda}_{LC}\end{aligned} \tag{4}$$

Equation (4) claims that $\boldsymbol{\Lambda}_{LC}\boldsymbol{\Lambda}_L = \boldsymbol{\Lambda}_L\boldsymbol{\Lambda}_{LC}$. The element form of this equation is,

$$\begin{bmatrix}\lambda_{LC1}\lambda_{L11} & \lambda_{LC1}\lambda_{L12} & \cdots & \lambda_{LC1}\lambda_{L1M}\\ \lambda_{LC2}\lambda_{L21} & \lambda_{LC2}\lambda_{L22} & \cdots & \lambda_{LC2}\lambda_{L2M}\\ \vdots & \vdots & \ddots & \vdots\\ \lambda_{LCM}\lambda_{LM1} & \lambda_{LCM}\lambda_{LM2} & \cdots & \lambda_{LCM}\lambda_{LMM}\end{bmatrix} = \begin{bmatrix}\lambda_{L11}\lambda_{LC1} & \lambda_{L12}\lambda_{LC2} & \cdots & \lambda_{L1M}\lambda_{LCM}\\ \lambda_{L21}\lambda_{LC1} & \lambda_{L22}\lambda_{LC2} & \cdots & \lambda_{L2M}\lambda_{LCM}\\ \vdots & \vdots & \ddots & \vdots\\ \lambda_{LM1}\lambda_{LC1} & \lambda_{LM2}\lambda_{LC2} & \cdots & \lambda_{LMM}\lambda_{LCM}\end{bmatrix} \tag{5}$$

To achieve the equivalence in (5), it requires that $\lambda_{Lij}\left(\lambda_{LCi}-\lambda_{LCj}\right)=0$ for all $i \neq j$. For matrix $\boldsymbol{LC}$ with *M* different eigenvalues, all off-diagonal elements λ_{Lij} of matrix $\boldsymbol{\Lambda}_L$ equal to zero, which claims that matrix $\boldsymbol{\Lambda}_L$ is a diagonal matrix. Similarly, matrix $\boldsymbol{C}$ can be diagonalized as $\boldsymbol{\Lambda}_C = \boldsymbol{T}_u^T\boldsymbol{C}\boldsymbol{T}_u$.

Note that, here the eigenvalues for matrix $\boldsymbol{LC}$ should be different. For a transposed line, this assumption is not satisfied and the counter-example that the matrix $\boldsymbol{\Lambda}_L$ is not diagonal matrix can be easily found. However, for untransposed line in practice, this assumption is always satisfied [18].

Introduce matrices $\boldsymbol{T}_u$ and $\boldsymbol{T}_i$ into (1),

$$\begin{aligned}\boldsymbol{T}_u^{-1}\,\partial \boldsymbol{u}_p/\partial x + \boldsymbol{T}_u^{-1}\boldsymbol{L}\boldsymbol{T}_i\boldsymbol{T}_i^{-1}\,\partial \boldsymbol{i}_p/\partial t + \boldsymbol{T}_u^{-1}\boldsymbol{R}\boldsymbol{T}_i\boldsymbol{T}_i^{-1}\boldsymbol{i}_p = \boldsymbol{0}\\ \boldsymbol{T}_i^{-1}\,\partial \boldsymbol{i}_p/\partial x + \boldsymbol{T}_i^{-1}\boldsymbol{C}\boldsymbol{T}_u\boldsymbol{T}_u^{-1}\,\partial \boldsymbol{u}_p/\partial t + \boldsymbol{T}_i^{-1}\boldsymbol{G}\boldsymbol{T}_u\boldsymbol{T}_u^{-1}\boldsymbol{u}_p = \boldsymbol{0}\end{aligned} \tag{6}$$

Define the mode voltage vector as $\boldsymbol{u}_m = \boldsymbol{T}_u^{-1}\boldsymbol{u}_p$ and mode current vector as $\boldsymbol{i}_m = \boldsymbol{T}_i^{-1}\boldsymbol{i}_p$, ignore the off-diagonal elements of matrices $\boldsymbol{T}_u^{-1}\boldsymbol{R}\boldsymbol{T}_i$ as $\boldsymbol{\Lambda}_R$ and $\boldsymbol{T}_i^{-1}\boldsymbol{G}\boldsymbol{T}_u$ as $\boldsymbol{\Lambda}_G$ (since effects of those values are relatively small). The transmission line equation is decoupled into *M* independent equation sets as,

$$\begin{aligned}\partial \boldsymbol{u}_m(x,t)/\partial x + \boldsymbol{\Lambda}_L\,\partial \boldsymbol{i}_m(x,t)/\partial t + \boldsymbol{\Lambda}_R\boldsymbol{i}_m(x,t) = \boldsymbol{0}\\ \partial \boldsymbol{i}_m(x,t)/\partial x + \boldsymbol{\Lambda}_C\,\partial \boldsymbol{u}_m(x,t)/\partial t + \boldsymbol{\Lambda}_G\boldsymbol{u}_m(x,t) = \boldsymbol{0}\end{aligned} \tag{7}$$

B. Solution of Voltage Distribution with Bergeron Model

For the n$^{\text{th}}$ mode decoupled single-mode line, that is n$^{\text{th}}$ equation in (7) ($n=1,2,\cdots,M$ for the rest of the paper),

$$\begin{aligned}\partial u_n(x,t)/\partial x + L_n\,\partial i_n(x,t)/\partial t + R_n i_n(x,t) = 0\\ \partial i_n(x,t)/\partial x + C_n\,\partial u_n(x,t)/\partial t + G_n u_n(x,t) = 0\end{aligned} \tag{8}$$

where u_n and i_n are the n[th] elements in vectors $\boldsymbol{u}_m$ and $\boldsymbol{i}_m$; L_n, R_n, C_n and G_n are n[th] diagonal elements in matrices $\boldsymbol{\Lambda}_L$, $\boldsymbol{\Lambda}_R$, $\boldsymbol{\Lambda}_C$ and $\boldsymbol{\Lambda}_G$, respectively.

The Bergeron model describes the relationship between the voltages and currents at terminals of a transmission line with certain length l [19]. It first ignores the terms with R_n and G_n in (8) to find the analytical solution for a lossless transmission line. Afterwards, the effect of resistance is considered by adding lumped resistors at the terminals and the mid-point of the line. The conductance is typically ignored. With the analytical solution of the lossless line and the consideration of lumped resistors, the Bergeron model gives the solution of (8),

$$\begin{aligned} i_{kn}(t) &= 1/Z_n \cdot u_{kn}(t) - (1+h_n)/2 \cdot \left[1/Z_n \cdot u_{mn}(t-\tau_n) \right. \\ &\left. + h_n i_{mn}(t-\tau_n)\right] - (1-h_n)/2 \cdot \left[1/Z_n \cdot u_{kn}(t-\tau_n) + h_n i_{kn}(t-\tau_n)\right] \\ i_{mn}(t) &= 1/Z_n \cdot u_{mn}(t) - (1+h_n)/2 \cdot \left[1/Z_n \cdot u_{kn}(t-\tau_n) \right. \\ &\left. + h_n i_{kn}(t-\tau_n)\right] - (1-h_n)/2 \cdot \left[1/Z_n \cdot u_{mn}(t-\tau_n) + h_n i_{mn}(t-\tau_n)\right] \end{aligned} \tag{9}$$

where $i_{kn}(t)$, $u_{kn}(t)$, $i_{mn}(t)$ and $u_{mn}(t)$ denote the currents and voltages at terminals of transmission line as $i_{kn}(t) = i_n(0,t)$, $i_{mn}(t) = -i_n(l,t)$, $u_{kn}(t) = u_n(0,t)$ and $u_{mn}(t) = u_n(l,t)$. $\tau_n = l\sqrt{L_n C_n}$, $Z_n = \sqrt{L_n/C_n} + lR_n/4$, $h_n = \left(\sqrt{L_n/C_n} - lR_n/4\right) \Big/ \left(\sqrt{L_n/C_n} + lR_n/4\right)$.

In purpose of solving the voltage distribution through the entire transmission line, express the voltage at one terminal of the line with the voltage and current at another terminal,

$$\begin{aligned} u_{mn}(t) &= 2Z_n \Big/ (1+h_n)^2 \cdot \left[1/Z_n \cdot u_{kn}(t+\tau_n) - i_{kn}(t+\tau_n)\right] \\ &-(1-h_n/1+h_n)^2 \cdot u_{kn}(t) - 2h_n(1-h_n) \Big/ (1+h_n)^2 \cdot Z_n i_{kn}(t) \\ &+2h_n^2 \Big/ (1+h_n)^2 \cdot Z_n \left[1/Z_n \cdot u_{kn}(t-\tau_n) + h_n \cdot i_{kn}(t-\tau_n)\right] \end{aligned} \tag{10}$$

Afterwards, vary the length of calculated transmission line in the range of $(0, l]$, the voltage distribution through the entire line is calculated from the voltage and current at one terminal.

III. Fault Location Algorithm

This section gives the fault location algorithm with calculated voltage distribution using (10). With equation (10), two voltage distribution curves can be calculated in each mode, one using the measurements at terminal k and another using the measurements at terminal m. Here the mode considered for fault location algorithm is denoted as mode f In the transformation matrix, the summation of the elements in the row corresponding to this mode should be close to zero. In this case, this mode has the physical meaning of the "line mode", which can minimize the influence of earth return and achieve high accuracy of fault location. On the other hand, the five-phase transmission line or even higher dimensional system could have more than one "line mode". In this paper, the mode f is selected according to the following criterion. For line to ground faults, choose the line mode where the faulted phase has the greatest contribution in the corresponding row. For line to line faults, choose the line mode where the coefficients for two phases are the closest to opposite numbers in the corresponding row.

For the chosen mode f, the intersection point of two calculated voltage distribution curves shows the fault location. To further improve the accuracy of the fault location, the summation of the voltage distribution curve at each time step is introduced for the fault location algorithm [5]. The x that minimizes following function gives the fault location,

$$\sum_{t=t_1}^{t_2} \left| u_f{}^k(x,t) - u_f{}^m(x,t) \right| \tag{11}$$

where $u_f{}^k(x,t)$ and $u_f{}^m(x,t)$ are the mode f voltage distributions calculated with measurements at terminals k and m respectively, interval $[t_1, t_2]$ is the summation window.

Here with the available measurement data window of $[0, t_f]$, the voltage distribution calculated through entire line is only between interval $[\tau_l, t_f - \tau_l]$ with (10). So the summation window is $[\tau_l, t_f - \tau_l]$.

IV. Numerical Experiments

In this section, a five-phase transmission line corridor, which includes a two-phase DC transmission line and a three-phase AC transmission line, is considered to verify the effectiveness of the proposed method. Beside the proposed fault location algorithm, the following two existing fault location methods are also considered to **show the importance of modeling the integrated coupled transmission line corridor** instead of modeling the two circuits (AC and DC circuit) independently and neglecting the effect of mutual coupling. Both existing methods use the Bergeron model to calculate the voltage distribution and to achieve voltage method fault location. However, one existing method only considers the DC line into the system and uses the eigenvalue decomposition to decouple the two dimensional system, the other one existing method only considers the AC line into the system and uses the eigenvalue decomposition to decouple the three dimensional system.

The example test system is shown in Figure 2(a). The transmission line is simulated using frequency dependent (phase) model in PSCAD/EMTDC. The tower structures for both DC line and AC line are shown in Figure 2 (b) (phases 1, 2 and 3, 4, 5 represent negative pole, positive pole of the DC line, and phases A, B, C of the AC line, respectively). The lengths of both DC line and AC line are 200 km. The ± 320 kV DC line is connected to the converter stations modular multilevel converter (MMC) 1 and MMC 2. The 230 kV AC line is directly connected to the AC sources. The five-phase instantaneous measurements of voltages and currents are installed at both terminals. The sampling rate is 100 kilo-samples per second. The data window is 5 ms.

Eight groups of fault events are considered: phase 2 to 3 faults, phases 2 and 3 to ground faults, phase 2 to ground low impedance and high impedance faults, phase 1 to 2 faults, phase 3 to ground low impedance and high impedance faults, and phase 4 to 5 faults. Each group of events are simulated with different fault impedances and fault locations. After applying the eigenvalue decomposition, the inverse of voltage eigenmatrix and the summation of each row are,

$$\boldsymbol{T}_u^{-1} = \begin{bmatrix} 0.6463 & 0.4627 & -0.1562 & -0.3893 & -0.4398 \\ -0.4129 & -0.4055 & -0.4727 & -0.4572 & -0.4833 \\ 0.2252 & -0.0594 & -0.6279 & -0.2107 & 0.7132 \\ 0.6032 & -0.7653 & 0.2189 & 0.0055 & -0.0594 \\ -0.1128 & 0.0192 & 0.5350 & -0.7731 & 0.3233 \end{bmatrix}, \text{sum}\left(\boldsymbol{T}_u^{-1}\right) = \begin{bmatrix} 0.1237 \\ -2.2317 \\ 0.0403 \\ 0.0030 \\ -0.0084 \end{bmatrix}.$$

One can observe that modes 4 and 5 are line modes. Choose the mode according to the criterion mentioned in section III. The specific mode chosen for fault location with each fault type is shown in Table 1.

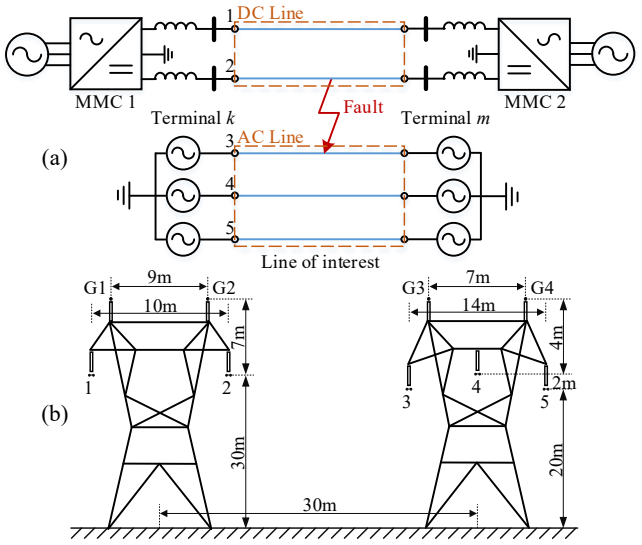

Figure. 2. Test system, (a) five-phase transmission line corridor and (b) tower structure of the system

Table. 1. Chosen mode for fault location with each fault type

Fault type	Chosen mode
Phase 2 to 3 faults	Mode 5
Phases 2 and 3 to ground faults	Mode 5
Phase 2 to ground faults	Mode 4
Phase 1 to 2 faults	Mode 5
Phase 3 to ground faults	Mode 5
Phase 4 to 5 faults	Mode 4

Figure 3 shows the absolute fault location errors with different fault types and different methods. Black line shows the results with the proposed method that considers a 5-phase model, red line shows the results that only consider a 2-phase model of the DC line, blue line shows the results that only consider a 3-phase model of the AC line. Here the method with only the AC line fails in locating faults occurring only in DC lines; the method with only DC line fails in locating faults occurring only in AC lines. Therefore, such results are not demonstrated in the following figures.

Group A: Phase 2 to 3 faults

Phases 2 to 3 faults are faults between DC line and AC line. The fault location results with three methods are shown in Figure 3 (a). The average and maximum absolute errors of the method with 5-phase model with 0.01, 1 and 2 ohm fault impedances are 0.12%, 0.13%, 0.15%, and 0.25%, 0.35%, 0.45%, respectively. The average and maximum absolute errors of the method with 2-phase model with 0.01, 1 and 2 ohm fault impedances are 0.45%, 0.45%, 0.45%, and 1.85%, 1.85%, 1.90%, respectively. The average and maximum absolute errors of the method with 3-phase model with 0.01, 1 and 2 ohm fault impedances are 0.38%, 0.36%, 0.35%, and 1.40%, 1.25%, 1.20%, respectively.

Group B: Phases 2 and 3 to ground faults

Phases 2 and 3 to ground faults are also faults between DC line and AC line. The fault location results with three methods are shown in Figure 3 (b). The average and maximum absolute errors of the method with 5-phase model with 0.01, 1 and 2 ohm fault impedances are 0.05%, 0.05%, 0.05%, and 0.10%, 0.10%, 0.10%, respectively. The average and maximum absolute errors of the method with 2-phase model with 0.01, 1 and 2 ohm fault impedances are 0.24%, 0.25%, 0.25%, and 1.10%, 1.15%, 1.15%, respectively. The average and maximum absolute errors of the method with 3-phase model with 0.01, 1 and 2 ohm fault impedances are 0.16%, 0.17%, 0.18%, and 0.40%, 0.40%, 0.40%, respectively.

Group C: Phase 2 to ground lowimpedance faults

Besides the faults between DC line and AC line, the faults in each single circuit are also studied. Phase 2 to ground faults are single pole to ground faults in DC line. The fault location results with two methods are shown in Figure 3 (c). The average and maximum absolute errors of the method with 5-phase model with 0.01, 1 and 2 ohm fault impedances are 0.10%, 0.14%, 0.16%, and 0.20%, 0.35%, 0.65%, respectively. The average and maximum absolute errors of the method with 2-phase model with 0.01, 1 and 2 ohm fault impedances are 0.32%, 0.31%, 0.30%, and 1.60%, 1.60%, 1.60%, respectively.

Group D: Phase 2 to ground high impedance faults

The fault location results for Phase 2 to ground high fault impedance faults with two methods are shown in Figure 3 (d). The average and maximum absolute errors of the method with 5-phase model with 10, 100 and 200 ohm fault impedances are 0.16%, 0.64%, 0.49%, and 0.70%, 1.60%, 1.90%, respectively.

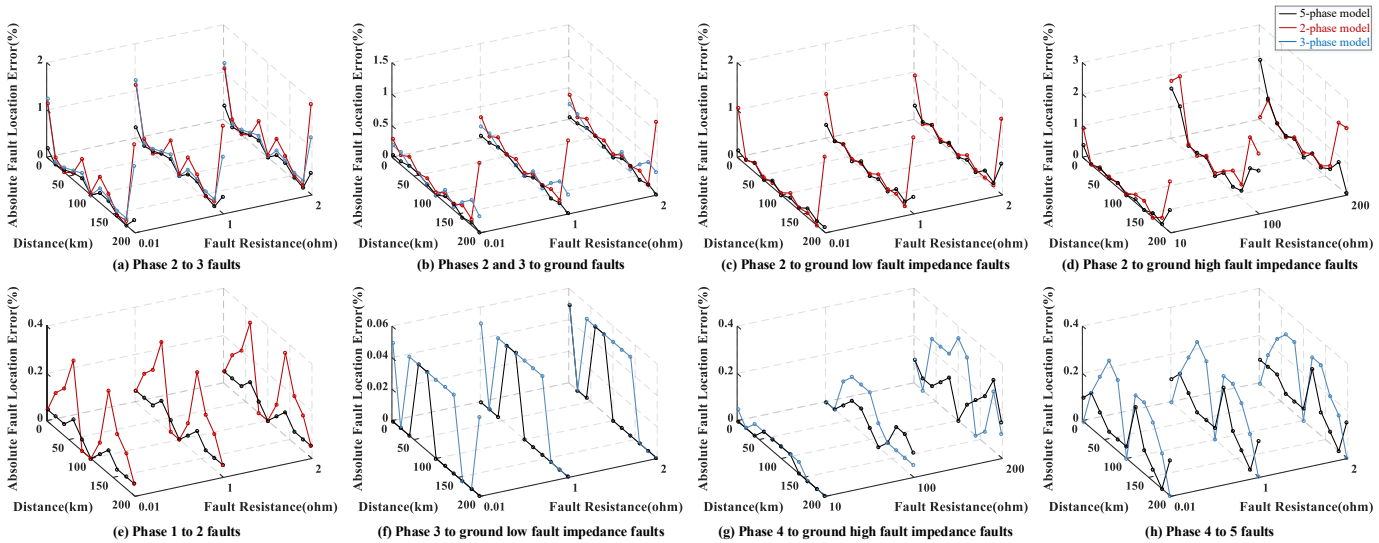

Figure. 3. Absolute fault location errors with different fault types and different methods

The average and maximum absolute errors of the method with 2-phase model with 0.01, 1 and 2 ohm fault impedances are 0.34%, 0.96%, 0.65%, and 1.60%, 2.20%, 2.10%, respectively.

Group E: Phase 1 to 2 faults

Phase 1 to 2 faults are pole to pole faults in DC line. The fault location results with two methods are shown in Figure 3 (e). The average and maximum absolute errors of the method with 5-phase model with 0.01, 1 and 2 ohm fault impedances are 0.05%, 0.05%, 0.05%, and 0.10%, 0.10%, 0.10%, respectively. The average and maximum absolute errors of the method with 2-phase model with 0.01, 1 and 2 ohm fault impedances are 0.15%, 0.15%, 0.15%, and 0.35%, 0.35%, 0.35%, respectively.

Group F: Phase 3 to ground low impedance faults

For the faults only in AC line, phase 3 to ground faults are single phase to ground faults in AC line. The fault location results with two methods are shown in Figure 3 (f). The average and maximum absolute errors of the method with 5-phase model with 0.01, 1 and 2 ohm fault impedances are 0.01%, 0.01%, 0.01%, and 0.05%, 0.05%, 0.05%, respectively. The average and maximum absolute errors of the method with 3-phase model with 0.01, 1 and 2 ohm fault impedances are 0.04%, 0.03%, 0.03%, and 0.05%, 0.05%, 0.05%, respectively.

Group G: Phase 4 to ground high impedance faults

The fault location results for Phase 3 to ground high fault impedance faults with two methods are shown in Figure 3 (g). The average and maximum absolute errors of the method with 5-phase model with 10, 100 and 200 ohm fault impedances are 0.02%, 0.07%, 0.12%, and 0.05%, 0.15%, 0.30%, respectively. The average and maximum absolute errors of the method with 3-phase model with 0.01, 1 and 2 ohm fault impedances are 0.03%, 0.10%, 0.17%, and 0.05%, 0.20%, 0.35%, respectively.

Group H: Phase 4 to 5 faults

Phase 4 to 5 faults are phase to phase faults in AC line. The fault location results with two methods are shown in Figure 3 (h). The average and maximum absolute errors of the method with 5-phase model with 0.01, 1 and 2 ohm fault impedances are 0.10%, 0.10%, 0.09%, and 0.25%, 0.25%, 0.25%, respectively. The average and maximum absolute errors of the method with 3-phase model with 0.01, 1 and 2 ohm fault impedances are 0.19%, 0.19%, 0.18%, and 0.35%, 0.35%, 0.30%, respectively.

For each type of fault, the proposed method shows higher fault location accuracy compare to the two existing methods that neglect the mutual coupling effect between AC and DC lines. Therefore, the modeling of the integrated coupled transmission line corridors does consider the mutual influence of lines in parallel in fault location application. However for the proposed method, there are still some errors. This is probably because the frequency dependency of the line parameters is not considered in the modeling procedure of the proposed method.

V. Conclusion

This paper proposes a time domain fault location algorithm for untransposed multi-phase transmission line corridors with distributed parameter model. The eigenvalue decomposition is applied to decouple the multi-phase system and the Bergeron model is applied to solve the voltage distribution and to determine the fault location. The specific application of the proposed method for a five-phase AC/DC line corridor shows higher fault location accuracy compared to fault location results without considering the mutual coupling effect between AC and DC systems, with only 5 ms data window. Nevertheless, although the proposed method is only suitable for untransposed lines, the partially transposed transmission lines in practice are actually constructed with several sections of untransposed lines that result in a nonhomogeneous untransposed line. The fault location for nonhomogeneous lines as well as the consideration of the frequency dependent parameters will be included in future publications.

References

[1] A. Gopalakrishnan, M. Kezunovic, S. M. McKenna and D. M. Hamai "Fault location using the distributed parameter transmission line model", *IEEE Trans. Power Deliv.*, Vol. 15, No. 4, pp. 1169-1174, Oct. 2000.

[2] C.Y. Evrenosoglu, A. Abur, "Traveling Wave Based Fault Location for Teed Circuits", *IEEE Trans. Power Deliv.*, Vol. 20, No. 2, pp. 1115–1121, Apr. 2005.

[3] Y. Liu, A. P. Meliopoulos, Z. Tan, L. Sun and R. Fan, "Dynamic State Estimation-Based Fault Locating on Transmission Lines", *IET Gener. Transm. Distrib.*, Vol. 11, No. 17, pp. 4184-4192, Nov. 2017.

[4] R. Fan, Y. Liu, R. Huang, R. Diao and S. Wang, "Precise Fault Location on Transmission Lines Using Ensemble Kalman Filter", *IEEE Trans. Power Del.*, Vol. 33, No. 6, pp. 3252-3255, Dec. 2018.

[5] Q. C. Zhang, Y. Zhang, and W. N. Song, "Fault location of two-parallel transmission line for nonearth fault using one-terminal data," *IEEE Trans. Power Del.*, vol. 14, no. 3, pp. 863–867, Jul. 1999.

[6] T. Funabashi, H. Otoguro, and Y. Mizuma, "Digital fault location for parallel double-circuit multi-terminal transmission lines," *IEEE Trans. Power Del.*, vol. 15, no. 2, pp. 531–537, Apr. 2000.

[7] J. L. Suonan, Y. P. Wu, and G. B. Song, "New accurate fault location algorithm for parallel lines on the same tower based on distributed parameter," in *Proc. Chinese Society Electrical Engineering*, vol. 23, 2003, pp. 39–43.

[8] C. Chen, C. Liu and J. Jiang, "A new adaptive PMU based protection scheme for transposed/untransposed parallel transmission lines," in *IEEE Trans. Power Del.*, vol. 17, no. 2, pp. 395-404, April 2002.

[9] G. Song, J. Suonan, Q. Xu, P. Chen and Y. Ge, "Parallel transmission lines fault location algorithm based on differential component net," in *IEEE Trans. Power Del.*, vol. 20, no. 4, pp. 2396-2406, Oct. 2005.

[10] Y. Yang, J. Lu and Y. Lei, "A Calculation Method for the Electric Field Under Double-Circuit HVDC Transmission Lines," in *IEEE Trans. Power Del.*, vol. 23, no. 4, pp. 1736-1742, Oct. 2008.

[11] Y. Qiu, H. Li, L. Guo, J. Wu and Y. Liang, "A fault location method for double-circuit HVDC transmission lines on the same tower based on mixed modulus," *2015 IEEE Eindhoven PowerTech*, Eindhoven, 2015, pp. 1-5.

[12] Y. Ma, H. Li, J. Hu, J. Wu and G. Wang, "Analysis of travelling wave protection criterion performance for double-circuit HVDC," *2013 IEEE PES Asia-Pacific Power and Energy Engineering Conference (APPEEC)*, Kowloon, 2013, pp. 1-5.

[13] Y. Ma, H. Li, G. Wang and J. Wu, "Fault Analysis and Traveling-Wave-Based Protection Scheme for Double-Circuit LCC-HVDC Transmission Lines With Shared Towers," in *IEEE Trans. Power Del.*, vol. 33, no. 3, pp. 1479-1488, June 2018.

[14] J. Tang et al., "Analysis of Electromagnetic Interference on DC Line From Parallel AC Line in Close Proximity," in *IEEE Trans. Power Del.*, vol. 22, no. 4, pp. 2401-2408, Oct. 2007.

[15] Y. Yang, J. Lu and Y. Lei, "A Calculation Method for the Hybrid Electric Field Under UHVAC and UHVDC Transmission Lines in the Same Corridor," in *IEEE Trans. Power Del.*, vol. 25, no. 2, pp. 1146-1153, April 2010.

[16] H. Ding, Y. Zhang, A. M. Gole, D. A. Woodford, M. X. Han and X. N. Xiao, "Analysis of Coupling Effects on Overhead VSC-HVDC Transmission Lines From AC Lines With Shared Right of Way," in *IEEE Trans. Power Del.*, vol. 25, no. 4, pp. 2976-2986, Oct. 2010.

[17] J. Schindler, C. Romeis and J. Jaeger, "Secondary Arc Current During DC Auto Reclosing in Multisectional AC/DC Hybrid Lines," in *IEEE Trans. Power Del.*, vol. 33, no. 1, pp. 489-496, Feb. 2018.

[18] L. M. Wedepohl, "Application of matrix methods to the solution of travelling-wave phenomena in polyphase systems," in *Proc. Inst. Elect. Eng.*, vol. 110, no. 12, pp. 2200-2212, December 1963.

[19] H. W. Dommel, "Digital computer solution of electromagnetic transients in single- and multiphase networks," in IEEE Trans. on Power Apparatus and Systems, vol. PAS-88, no. 4, pp. 388–399, April 1969.